Pergamon

Int. J. Heat Mass Transfer. Vol. 39, No. 2, pp. 347–354, 1996

0017-9310/96 $9.50 + 0.00

0017-9310(95)00116-6

Effects of a moving thermal wave on Bénard convection in a horizontal saturated porous layer

M. MAMOU, L. ROBILLARD,† E. BILGEN and P. VASSEUR
Ecole Polytechnique, University of Montreal, C.P 6079 Succ 'A', Montreal, P.Q., Canada H3C 3A7

(*Received* 11 *May* 1993 *and in final form* 3 *March* 1995)

Abstract—A numerical study is carried out on the natural convection taking place in a horizontal saturated porous layer. A sinusoidal temperature distribution, as a moving wave, is superposed on the hot temperature of the lower plate. The imposed wavelength of this perturbation is equal to the wavelength of incipient Bénard cells. For a given Rayleigh number R, results show that the Bénard cells move with the imposed wave if the velocity of the latter remains below a critical value. Beyond this critical value, there is still an entrainment of the cells, but at a much lower rate. Further, the cell motion is irregular and time periodic.

INTRODUCTION

The effects of temporal or spatial variations of the thermal boundary conditions in a horizontal fluid or saturated porous layers have received considerable attention in the last few years. A large part of the work has been focused on the effects of these variations considered as imperfections of small amplitude in classical stability problems.

Analytical studies of standing thermal waves of small amplitude superposed on the hot temperature of the lower wall and to the cold temperature of the upper wall have been published for both the fluid and the saturated porous layer. Kelly and Pal [1] and Pal and Kelly [2] have investigated the case of a fluid layer subjected to a spatial periodic temperature on its lower and upper boundaries. Their analysis was two-dimensional. Resonant ($k = k_C$) and non-resonant ($k \neq k_C$) wavelength excitations were considered. For $k \sim k_C$, multiple solutions were found to exist when the Rayleigh number was larger than the critical Rayleigh number for the existence of classical Bénard cells ($R > R_C$). However their stability analysis indicates that all solutions are unstable to a phase shift in the horizontal direction, except for the solution with maximum amplitude. More recently, investigations for the case of a saturated porous layer subjected to near-resonant and non-resonant thermal forcing were conducted by Rees and Riley [3, 4]. Their studies focused on the stability of the resulting two-dimensional rolls to three-dimensional disturbances.

Relatively few studies have been done on temporal variations of the thermal boundary conditions and their effects on classical Bénard cells. A general survey of time-periodic flow problems and their stability has been published by Davis [5], part of this work being devoted to thermal instability. More specifically, Schhuon and Caltagirone [6] have considered theoretically and experimentally the case of a horizontal porous layer with a timewise periodic temperature imposed on the lower boundary. Analytical results provide the critical Darcy–Rayleigh number as a function of the amplitude and wavenumber of the imposed time-dependent disturbance.

A few studies of moving thermal waves in horizontal fluid layers have been conducted in the past [7–9]. The fluid motion was induced exclusively by the periodic travelling thermal wave. Such a thermal wave can be produced either by boundary heating [9] or from a time-dependent source term [8]. The work done by Young *et al.* [9] is based on a numerical approach and involves a finite amplitude convection. It confirmed the existence of a net mean flow induced by the moving wave, as predicted analytically by previous workers.

Concerning the practical aspects of the present work, Whitehead [10] mentioned that studies of moving thermal waves have many obvious applications in geophysics, biology and engineering. Also, as stated by Young *et al.* [9], those studies have interest as pure fluid dynamic problem. Following the investigations by Young *et al.* [9] and Whitehead [10], many analyses have been done on the effects of small imperfections on classical flows, such as Bénard convection. The results of the studies are of considerable interest in the study of non-linear systems in general [3].

The objective of the present study was to investigate numerically the entrainment effect of a moving thermal wave on the Bénard cells in a horizontal saturated porous layer with zero net flow maintained between the two horizontal boundaries. The thermal wave takes the form of a sinusoidally distributed temperature superposed on the hot temperature of the lower boundary with a wavenumber equal to the critical wavenumber $k_C = \pi$. Moreover, we assume that the solution is periodic in the x direction, with a wave-

† Author to whom correspondence should be addressed.

NOMENCLATURE

f	arbitrary function, equation (13)
g	acceleration due to gravity [cm s^{-2}]
h'	thickness of the porous layer [cm]
k	dimensionless wavenumber, $2\pi/\hat{\lambda}$
K	permeability of the porous medium [cm^2]
k_C	critical wavenumber for classical Bénard cells
Nu	Nusselt number, equations (14) and (15)
R	Darcy–Rayleigh number, $g\beta K\Delta T'h'/\alpha\nu$
R_C	critical Rayleigh number
U'	velocity of imposed thermal wave [cm s^{-1}]
U	dimensionless velocity of the thermal wave, $\sigma U'h'/\alpha$
V	dimensionless instantaneous cell velocity in the x direction
$\bar{V}$	dimensionless time-averaged cell velocity in the x direction
t'	time [s]
T'	temperature [K]
T_{av}	dimensionless temperature averaged over the flow domain, equation (17)
$\Delta T'$	characteristic temperature [K]
u', v'	velocities in the x' and y' directions [cm s^{-1}]
x', y'	coordinates in the horizontal and vertical directions [cm].

Greek symbols

α	thermal diffusivity, $\kappa/(\rho c)_f$ [cm^2 s^{-1}]
β	thermal expansion coefficient [K^{-1}]
ε'	amplitude of imposed thermal wave [K]
κ	conductivity of saturated porous medium [cal cm^{-1} s^{-1} K^{-1}]
$\hat{\lambda}$	dimensionless wavelength
μ	dynamic viscosity of fluid [g cm^{-1} s^{-1}]
ν	kinematic viscosity of fluid [cm^2 s^{-1}]
ρ	density of fluid [g cm^{-3}]
$(\rho c)_f$	heat capacity of fluid [cal cm^{-3} K^{-1}]
$(\rho c)_p$	heat capacity of saturated porous medium [cal cm^{-3} K^{-1}]
σ	heat capacity ratio, $(\rho c)_p/(\rho c)_f$
τ	time period
φ	phase angle
Ψ'	stream function [cm^2 s^{-1}].

Subscripts

av	quantity averaged over the flow domain
ext	extremum quantity
l	refers to lower boundary
u	refers to upper boundary.

Superscripts

′	dimensional variable
*	refers to moving coordinate system.

length corresponding to the imposed perturbation. This may appear a bold assumption in the context of finite amplitude convection since it is generally admitted, from experiments and theoretical predictions, that the wavenumber is not a constant but depends on the Rayleigh number and possibly on the Prandtl number when inertia effects are present [11]. Thus one may therefore question the periodicity resulting from the interaction between an imposed periodic disturbance and finite amplitude Rayleigh–Bénard convection of potentially different wavelength. There is, however, some ground for the above assumption, which may be found in the context of a fluid layer. Firstly, past experiments by Chen and Whitehead [12] for the range $R_C < R < 2.5R_C$ indicate that a disturbance with an arbitrary wavenumber (not too far from k_C), imposed as a boundary condition, will promote a convective pattern corresponding to that wavenumber. Secondly, non-linear analyses [13] for finite amplitude convection with R slightly above R_C preclude the possibility of a mixed equilibrium containing both disturbances, i.e. only one will survive. It also appears from these studies that initial conditions strongly determine the precise wavenumber selected. In the present study the initial conditions are replaced by an imposed disturbance which is maintained indefinitely.

We assume here that the flow and temperature fields are two-dimensional in conformity with the two-dimensional disturbance. Furthermore, the problem is solved in a coordinate system moving at the velocity of the thermal wave. As seen from the moving reference frame, some similarity exists between the present problem and the mixed convection in a horizontal layer where heating elements are regularly spaced over the lower boundary. Tomimura and Fujii [14], Hasnaoui *et al.* [15] and, more recently, Tangborn [16] and Yücel *et al.* [17], have investigated this mixed convection problem for the case of a fluid medium. In particular, results from Hasnaoui *et al.* [15] show that, depending upon the intensity of the forced flow, two flow regimes may exist. At low Reynolds number, a steady state is possible for which the convective cells remain attached to the heating elements. Beyond a critical value, no steady state is possible. The cells are carried with the stream, periodically reinforced and weakened, according to their position along the lower boundary.

When handling the governing equations for a satu-

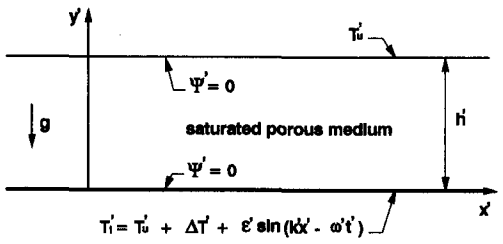

Fig. 1. Geometry of the problem.

rated porous medium in a coordinate system moving with respect to the solid matrix, one must account for the fact that the solid material has a heat capacity that may differ from the fluid itself and that it carries heat at a specific rate in its relative motion. A discussion on that matter may be found in refs. [18, 19].

GOVERNING EQUATIONS

The geometry considered is a two-dimensional fluid saturated porous layer of infinite extent bounded by two horizontal impermeable walls (see Fig. 1). T'_u is the cold uniform temperature of the upper wall and T'_l the hot temperature of the lower wall. T'_l is given by

$$T'_l = T'_u + \Delta T' + \varepsilon' \sin(k'x' - \omega' t'). \tag{1}$$

Equation (1) contains a disturbance in the form of a moving thermal wave of velocity $U' = \omega'/k'$ and of amplitude $\varepsilon' < \Delta T'$. The wavenumber k' is chosen to correspond to the critical wavenumber $k'_c = \pi/h'$ of classical Rayleigh–Bénard convection in a Darcy porous layer (resonant wavelength excitation).

It is assumed in the present study that the Boussinesq approximation holds and that all fluid and solid properties are constant, except for density in the buoyancy term. It is also assumed that dissipation effects are negligible. The basic set of equations expressing continuity, momentum and energy may then be reduced to the following:

$$\nabla^2 \Psi = -R \frac{\partial T}{\partial x} \tag{2}$$

$$u = \frac{\partial \Psi}{\partial y} \quad \text{and} \quad v = -\frac{\partial \Psi}{\partial x} \tag{3}$$

$$\frac{\partial T}{\partial t} + u\frac{\partial T}{\partial x} + v\frac{\partial T}{\partial y} = \frac{\partial^2 T}{\partial x^2} + \frac{\partial^2 T}{\partial y^2} \tag{4}$$

with boundary conditions

$$\left.\begin{array}{llll} y = 0 & \Psi = 0 & T = 1 + \varepsilon \sin k(x - Ut) \\ y = 1 & \Psi = 0 & T = 0 \end{array}\right\}. \tag{5}$$

Equations (2)–(5) have been reduced to dimensionless form by introducing the following scales:

$$\left.\begin{array}{ll} (x, y) = (x', y')/h' & t = t'\alpha/\sigma h'^2 \\ (u, v) = (u', v')h'/\alpha & \Psi = \Psi'/\alpha \\ T = (T' - T'_u)/\Delta T' & \Delta T' = T'_l - T'_u \\ R = \dfrac{g\beta K \Delta T' h'}{\alpha \nu} & U = U'\sigma h'/\alpha \end{array}\right\}. \tag{6}$$

In the above equations R and U are the Darcy–Rayleigh number and the dimensionless velocity of the thermal wave respectively.

Young *et al.* [9] have shown theoretically that a net flow could be induced in a fluid layer by a moving thermal wave. For the present problem, no such flow is possible since the integration over one wavelength $\lambda = k/2\pi$ of the horizontal momentum equation for a Darcy porous medium yields the following result

$$\int_0^\lambda u \, dx = 0 \tag{7}$$

which holds for any y.

Following the procedure used by Young *et al.* [9], we rewrite the governing equations in a frame of reference (x^*, y^*) moving with the imposed thermal wave. Whenever a steady state is possible in that frame of reference, it is concluded that Bénard cells are carried with the wave. We use the following relationships in equations (2)–(5):

$$\left.\begin{array}{l} x^* = x - Ut \\ u^* = u - U \\ \Psi^* = \Psi - Uy \\ \left.\dfrac{\partial T}{\partial t}\right|_{\text{moving frame}} = \left.\dfrac{\partial T}{\partial t}\right|_{\text{fixed frame}} + U\dfrac{\partial T}{\partial x} \end{array}\right\}. \tag{8}$$

Dropping the superscript asterisk from now on, the problem can be stated as follows:

$$\nabla^2 \Psi = -R \frac{\partial T}{\partial x} \tag{9}$$

$$u = \frac{\partial \Psi}{\partial y} \quad \text{and} \quad v = -\frac{\partial \Psi}{\partial x} \tag{10}$$

$$\frac{\partial T}{\partial t} + u\frac{\partial T}{\partial x} + v\frac{\partial T}{\partial y} = \frac{\partial^2 T}{\partial x^2} + \frac{\partial^2 T}{\partial y^2} \tag{11}$$

$$\left.\begin{array}{llll} y = 0 & \Psi = 0 & T = 1 + \varepsilon \sin kx \\ y = 1 & \Psi = -U & T = 0 \end{array}\right\}. \tag{12}$$

A coordinate system moving with respect to the porous matrix has already been used by Prats [18] for the mixed convection in a horizontal porous layer. Prats showed that the relative dimensional velocity between the porous matrix and the coordinate system had to be U'/σ (where U' was the mean velocity of the forced flow) in order to recover the equations solved by Lapwood [20] for free convection in a saturated porous medium. For the present problem, the relative dimensionless velocity is $U = U'\sigma h'/\alpha$. With this particular choice of U, σ does not need to be treated as an independent parameter. Thus, the num-

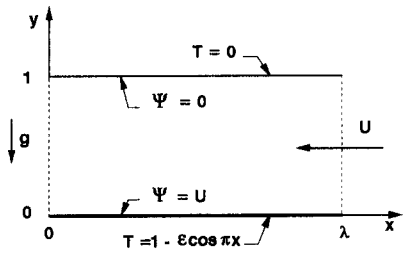

Fig. 2. Numerical flow domain.

ber of governing parameters is limited to three, namely the Rayleigh number R, the dimensionless velocity U and the amplitude ε of the disturbance.

The solution is assumed to be periodic in the x direction according to the wavenumber k_C. Consequently, the domain to be solved numerically may be restricted to the rectangular 'window' shown in Fig. 2 with periodic boundary conditions for the vertical boundaries of the form

$$f(x, y, t) = f(x+\lambda, y, t) \tag{13}$$

where f stands for any physical variable. For symmetry purposes in graphic representations of flow and temperature fields, the boundary condition $T(x, 0) = 1 - \varepsilon \cos kx$ is used instead of equation (12) in Fig. 2.

The Nusselt numbers relative to the upper and lower boundaries are defined, respectively, as

$$Nu_u = -\frac{1}{\lambda}\int_0^{\lambda} \left.\frac{\partial T}{\partial y}\right|_{y=0} \mathrm{d}x \tag{14}$$

$$Nu_l = -\frac{1}{\lambda}\int_0^{\lambda} \left.\frac{\partial T}{\partial y}\right|_{y=1} \mathrm{d}x. \tag{15}$$

For the unsteady convection, the energy balance leads to the following relationship

$$Nu_l - Nu_u = \frac{\partial T_{av}}{\partial t} \tag{16}$$

where T_{av} is the average temperature of the porous layer defined as

$$T_{av} = \frac{1}{\lambda}\int_0^1 \int_0^{\lambda} T \,\mathrm{d}x\,\mathrm{d}y. \tag{17}$$

NUMERICAL APPROACH

A finite difference method was used to solve governing equations (9)–(11) with boundary conditions (12) and (13). The entire domain (Fig. 2) was discretized with a uniform mesh size. An alternating direction implicit (ADI) method was used to solve equation (11). The Poisson equation (9) was solved by the method of successive over-relaxation. The advective terms were formulated by central differences.

The ADI method requires boundary conditions in the x and y directions. To take care of the periodicity conditions (13) prevailing at end points in the x direction, a partition procedure comparable with the one used by Phillips [21] was applied to the resulting matrices. Periodic boundary conditions allow the origin of the numerical domain to be at any position along the wavelength. However, the perfect permeability of the vertical boundaries makes the solution very sensitive, in the sense that a drift in the x direction automatically occurs for the slightest bias in the numerical scheme. To overcome that problem, the successive over-relaxation method was applied both in the positive and negative x directions and mean values were taken.

Preliminary tests on grid independence were done using various mesh sizes and it was found that a 41×41 grid was a good compromise between computer time and accuracy of the results for the range of parameters considered, $0 < R < 300$ and $0 \leqslant U \leqslant 6$. Other tests were also performed to ensure independence of the time increment. Based on the same considerations, time increments of 0.0005 and 0.001 were used for the numerical results.

With ε set to zero (Lapwood problem), the numerical code was checked to reproduce in a satisfactory way the functional dependence Nu vs R, as established theoretically and experimentally by many authors (see Cheng [22] and Caltagirone [23]). For instance, at $R = 200$, $Nu = 3.801$ and $\Psi_{ext} = 8.940$ were obtained for a bottom heated square cavity by the present study as compared with $Nu = 3.813$ and $\Psi_{ext} = 8.942$ from Caltagirone [23]. At $R = 300$ our results were $Nu = 4.501$ and $\Psi_{ext} = 11.392$. Those from Caltagirone [23] were $Nu = 4.523$ and $\Psi_{ext} = 11.405$. Results with ε set to zero were unaffected when a moving frame of reference (or equivalently a forced flow) was considered for the range $0 \leqslant U \leqslant 6$. Under the conditions $\varepsilon = 0$ and $U \neq 0$, the flow was unsteady periodic, the convective cells being carried along with the forced flow. The time-averaged cell velocity $\bar{V}$ was simply deduced from the time period τ characterizing the unsteady solution $\bar{V} = \lambda/\tau$ and it was found to be practically identical to $-U$ within 0.1%. The estimate of V, the time-dependent velocity of cells, was based on the x position of Ψ_{ext} at a given time. The estimate of that position has limitations inherent to the space discretization. Interpolation techniques were used in order to improve the accuracy.

RESULTS AND DISCUSSION

The present results cover the ranges $0 \leqslant R \leqslant 300$, $0 \leqslant U \leqslant 6$ and $0 \leqslant \varepsilon \leqslant 0.3$. All computations were done for $\lambda = 2$.

Standing thermal wave

(*a*) $\varepsilon = 0$. Without a thermal wave, a pure conduction state exists when the Rayleigh number R is between zero and a critical value $R_C = 4\pi^2$. That critical value correspond to the onset of the convective motion. The behavior of the system is depicted in Fig.

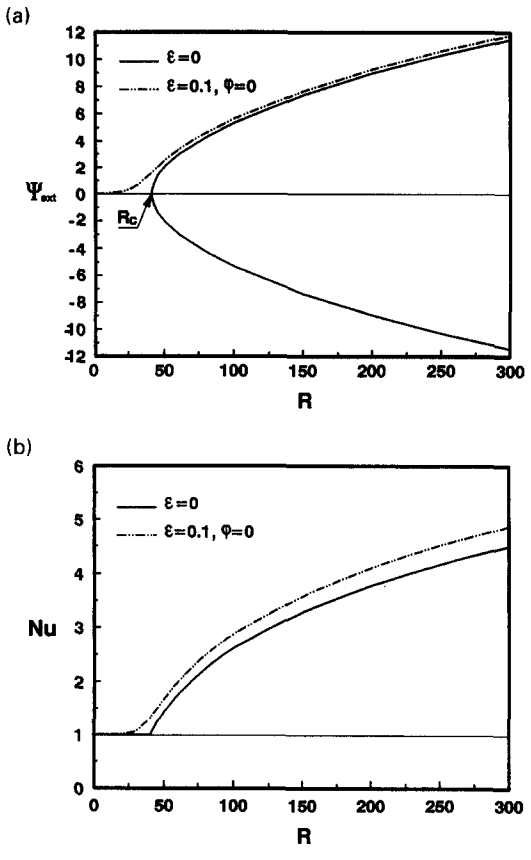

Fig. 3. Standing wave-multiple solutions: (a) Ψ_{ext} vs R; (b) Nu vs R.

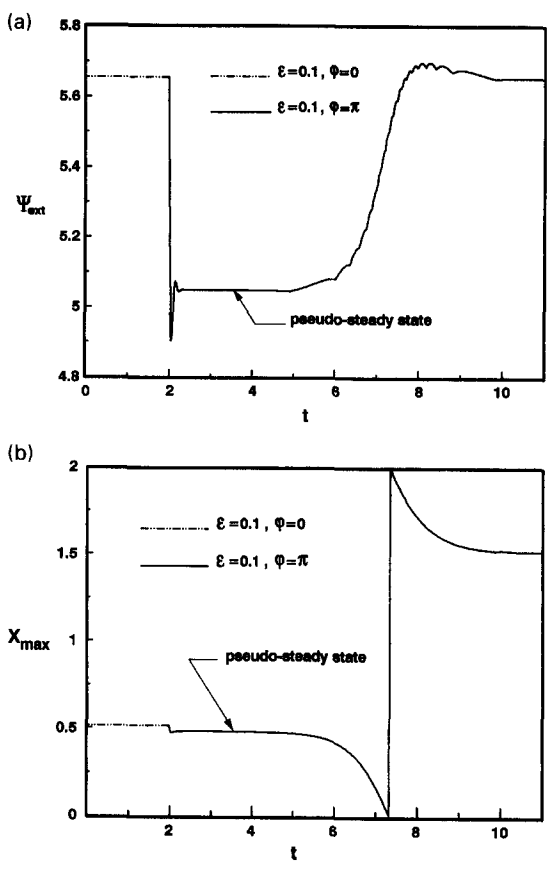

Fig. 4. Time dependence of extremum stream function Ψ_{ext} (a) and location X_{max} (b) of the clockwise cell.

3(a) and (b) where Ψ_{ext} is the extremum value of the stream function and $Nu = Nu_l = Nu_u$ is the overall Nusselt number. Ψ_{ext} is a measure of the intensity of convection.

The numerical results ($\varepsilon = 0$) define the parabolic type of curve expected in the neighborhood of R_C. At $R > R_C$, positive and negative branches correspond to clockwise and counterclockwise cells, respectively. Also, without a thermal wave there is no preferred location of the cells along the x direction in the numerical domain. This corresponds to the so-called horizontal isotropy of the Rayleigh–Bénard problem.

(*b*) $\varepsilon \neq 0$. When a standing thermal wave [$\varepsilon = 0.1$ in Fig. 3(a) and (b)] is superposed to the lower wall temperature, convective cells are found to exist along the layer even for $0 < R < R_C$. Those cells alternate from clockwise to counterclockwise motion and are always in phase (curve with phase angle $\varphi = 0$) with the thermal wave, the upward flow being located above the maximum temperature of the lower wall. When R is increased beyond R_C, no abrupt change is encountered, but Ψ_{ext} increases more rapidly and remains above the previous curve corresponding to classical Bénard cells. This solution branch is termed 'preferred' according to Ehrhard and Muller [24] or 'natural' according to Nield and Bejan [25], since numerical computations starting from the rest state always converge towards that branch.

A search for steady state solutions out of phase by 180° has been done numerically for the range $R_C < R < 300$. According to their theoretical investigation for a fluid layer, Kelly and Pal [1] predicted that such a solution is unstable to a phase shift. The present numerical results indicate that a comparable behavior occurs for the fluid-saturated porous layer. The search was done by starting the computation from initial conditions containing cells already out of phase by exactly 180° with respect to the imposed thermal wave. After a relatively short period of time for the initial transient, the system reaches an almost time independent state (pseudo-steady state); however, when the computation is pursued long enough, a horizontal drift of the cells gradually develops. This drift, which is almost imperceptible at first, is gradually amplified and the cells eventually move by one half wavelength to a final location where they are in phase with the imposed thermal wave. The behavior is depicted in Fig. 4(a) and (b) where Ψ_{ext} (clockwise cell) and X_{max} (horizontal position of Ψ_{ext}) are plotted as functions of time. The initial transient starts at $t = 2$ and the pseudo steady-state is reached at $t \simeq 2.15$. At $t \simeq 6.65$ the clockwise cell disappears at the left of the flow domain and reappears at the right.

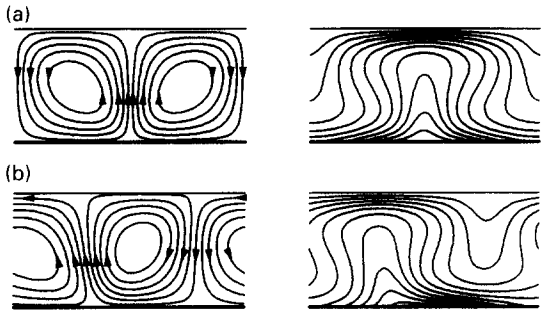

Fig. 5. Steady state flow and temperature fields, $R = 100$ and $\varepsilon = 0.3$: (a) $U = 0$, $\Psi_{max} = 6.231$, $\Psi_{min} = -6.231$, $Nu = 3.473$; (b) $U = 1.5$, $\Psi_{max} = 6.187$, $\Psi_{min} = -5.356$, $Nu = 3.012$.

Moving thermal wave $U \neq 0$

The problem may be considered from a coordinate system moving with the thermal wave in which case this latter becomes a standing wave and a net flow U towards the left is then imposed between the two boundaries (Fig. 2). As mentioned earlier, whenever a steady state solution is possible within that frame of reference, it means that the moving wave carries the cells with it in the original frame of reference (Fig. 1). The present investigation reveals that for a given pair of values R and ε there exists a critical velocity U_C beyond which no steady state is possible. This behavior of the system is shown in Figs. 5(a), (b) and 6 for which $R = 100$ and $\varepsilon = 0.3$ and $U = 0$, 1.5 and 2, respectively. The flow and temperature fields are given, respectively, by streamlines on the left and isotherms on the right. Also the thermal wave is symmetrically located with the maximum temperature at the center of the lower boundary shown in each figure.

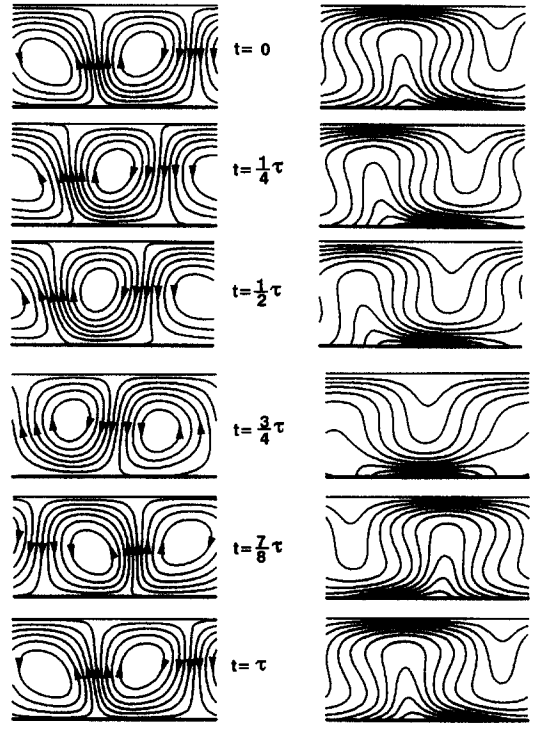

Fig. 6. Unsteady periodic flow and temperature fields at different time during one cycle ($R = 100$, $U = 2$, $\varepsilon = 0.3$ and $\tau = 1.976$).

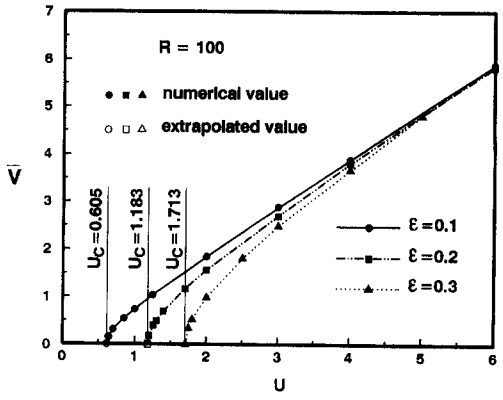

Fig. 7. Cell velocity in moving frame of reference as a function of U.

For $U = 0$, the symmetric flow pattern of Fig. 5(a) is obtained. It corresponds to the preferred branch already described and consists of two counter-rotating cells producing an upward flow in the mid region. The symmetry found in Fig. 5(a) is destroyed as U is increased progressively. This is illustrated in Fig. 5(b) ($U = 1.5$) where the convective cells are skewed and displaced downstream. However, a steady state may be reached as the convective cells remain attached to the thermal wave.

The case with $U = 2$ shown in Fig. 6 is beyond the threshold (from Fig. 7, $U_C = 1.713$ for $R = 100$ and $\varepsilon = 0.3$). A steady state solution is no more possible and, as observed from the second frame of reference, the cells are carried with the flow U in an irregular (time periodic) motion. Figure 6 shows the sequence of flow and temperature fields occurring at different times during one full period $\tau = 1.976$. The shape and intensity of the cells are changing as they move towards the left.

The time-averaged velocity of the cells, $\bar{V}$, as seen from the moving coordinate system, is plotted in Fig. 7 as a function of U for $R = 100$ and $\varepsilon = 0.3$, 0.2 and 0.3. The threshold values $U_C \approx 0.605$, 1.183 and 1.713 are obtained by extrapolation of the numerical results. With U increasing to large values, it may also be deduced from Fig. 7 that $\bar{V}/U$ tends asymptotically towards unity. Thus, for an observer at rest with respect to the porous matrix (original coordinate system), the entrainment of the convective cells by the moving thermal wave is gradually reduced to zero with increasing U.

Threshold values U_C have been determined for the range $60 < R < 300$ and for the three amplitudes $\varepsilon = 0.1$, 0.2 and 0.3. Results are shown in Fig. 8. The lower limit $R_C = 4\pi^2$ for the existence of classical Bénard cells has been identified in the figure. The

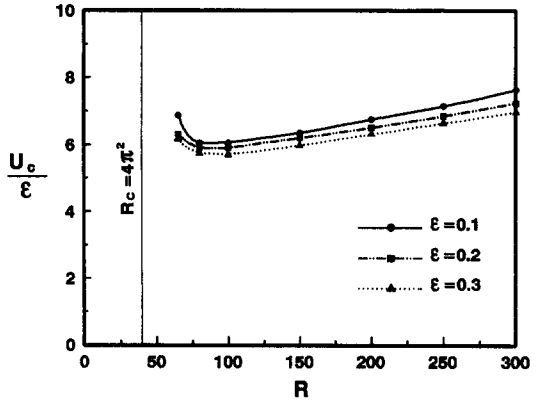

Fig. 8. Critical thermal wave velocity function of R.

amplitude ε is a parameter that influences strongly the value of U_C and it was found advantageous to plot the ratio U_C/ε as a function of R since the numerical results corresponding to different ε almost collapse together. U_C/ε is minimum at $R \approx 100$ and increases in both positive and negative directions. With R decreasing from 100 to R_C, the intensity of the convective cells depends more and more upon the thermal wave itself and this explains why the cells can be carried with it more easily. On the other hand, for the range $R > 100$, the reason for Bénard cells to develop a stronger bound with the thermal wave is not physically obvious. For that range, the trend is similar to the one observed by Hasnaoui *at al.* [15] in their numerical study of mixed convection in a horizontal channel heated periodically from below.

The unsteady (periodic) state obtained for $U > U_C$, as observed from the moving coordinate system, is characterized by an irregular cell motion relative to the thermal wave. This behavior is shown in Fig. 9(a) where V is given as a function of time. Other flow and heat transfer parameters such as the extrema of the stream function shown in Fig. 9(b) or the Nusselt numbers Nu_u and Nu_l, shown in Fig. 9(c), are also characterized by a time periodic dependence.

A particular feature of the unsteady periodic state is the irregular (cyclic) way by which heat is transferred from the lower boundary to the upper boundary. It may be seen in Fig. 9(c) that Nu_u and Nu_l are out of phase in their cyclic variations. Thus the heat content of the saturated porous layer must also be time-dependent. During one cycle, part of the heat from the lower boundary is at first stored within the layer and then released through the upper boundary. At each time step, in the numerical computation, the energy balance expressed by equation (16) is satisfied to a high degree of accuracy by the present numerical code, as can be seen in Fig. 10 where the left and right terms of equation (16), shown respectively by dotted and solid lines, have been computed separately for the case $R = 100$, $U = 6$ and $\varepsilon = 0.3$.

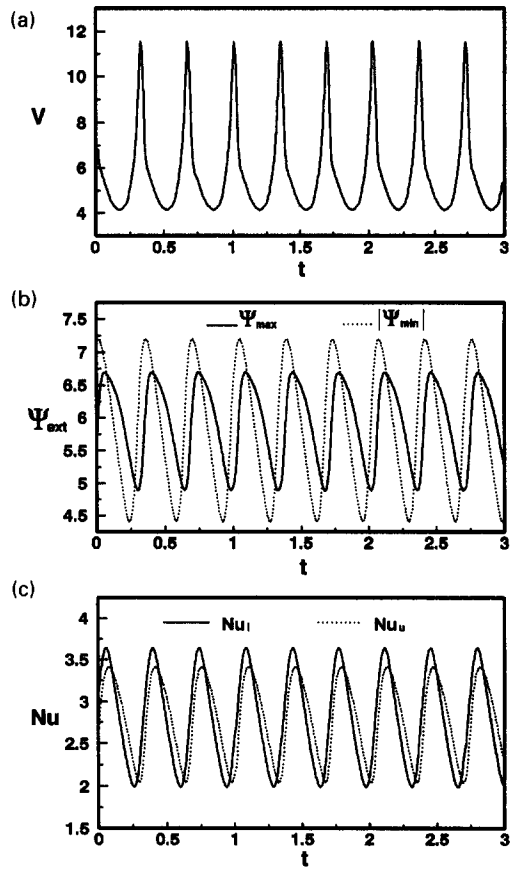

Fig. 9. Time dependence of V, Ψ_{max}, Ψ_{min}, Nu_u and Nu_l ($R = 100$, $U = 6$ and $\varepsilon = 0.3$).

CONCLUSIONS

The behavior of convective cells in a horizontal saturated porous layer when a moving thermal wave is superposed on the hot temperature of the lower boundary has been investigated numerically for the range $R_C < R < 7.5R_C$. The wavelength of the modulation were set equal to the critical wavelength of the incipient Bénard cells and we assumed that the

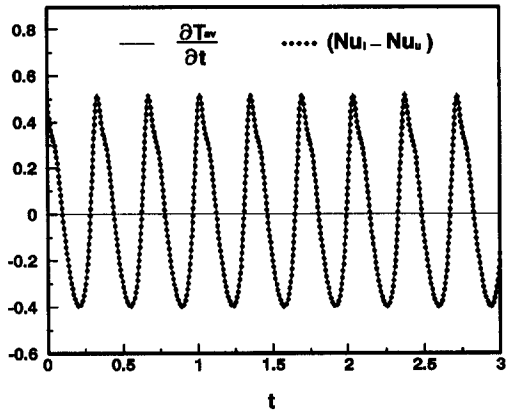

Fig. 10. Energy balance ($R = 100$, $U = 6$ and $\varepsilon = 0.3$).

resulting periodicity of the solution would correspond to the imposed disturbance, thus reducing our solution domain to one wavelength.

The main finding is the occurrence of a threshold separating steady from unsteady time periodic solutions. That threshold depends strongly upon the amplitude ε of the thermal wave and weakly upon the Rayleigh number. Below the threshold, the behavior of the cells gives rise to a steady state solution when the governing equations are solved in a coordinate system moving with the thermal wave. The cells are then carried at the velocity of the imposed thermal wave. Above the threshold, the cells move in a quite irregular way with a time-averaged velocity much lower than the thermal wave. An unsteady periodic state occurs for which all physical parameters are characterized by a cyclic time dependence. An important feature resulting from this irregular motion is the release of the heat by bursts from the saturated porous layer through the upper boundary.

The limit case of a thermal wave at rest with respect to the porous matrix was first considered. For Rayleigh numbers larger than R_C, two distinct solutions were discussed, one with the cells in phase with the thermal wave, i.e. with upward flows above the locations of maximum temperature, and the other with cells out of phase by 180°. The first type is stable and belongs to the preferred branch of a bifurcation at R_C, the thermal wave acting as an imperfection brought to the system. The second type of solution forms an isolated branch and is unstable to a phase shift.

Acknowledgements – Financial support by the Natural Sciences and Engineering Research Council of Canada, FCAR, Province of Quebec and Ministry of High Education of Algeria is acknowledged.

REFERENCES

1. R. E. Kelly and D. Pal, Thermal convection with spatially periodic boundary conditions: resonant wavelength excitation, *J. Fluid Mech.* **86,** 433–456 (1978).
2. D. Pal and R. E. Kelly, Thermal convection with spatially periodic nonuniform heating: resonant wavelength excitation, *Proceeding of the Sixth International Heat Transfer Conference*, Vol. 2, pp. 235–238, Toronto. Hemisphere, New York (1978).
3. D. A. S. Rees and D. S. Riley, The effects of boundary imperfections on convection in a saturated porous layer: near-resonant wavelength excitation, *J. Fluid Mech.* **199,** 133–154 (1989).
4. D. A. S. Rees and D. S. Riley, The effects of boundary imperfections on convection in a saturated porous layer: non-resonant wavelength excitation, *Proc. R. Soc. Lond., A* **421,** 303–339 (1989).
5. S. H. Davis, The stability of time periodic flow, *A. Rev. Fluid Mech.* **8,** 57–74 (1976).
6. B. Schhuon and J. P. Caltagirone, Stability of a horizontal porous layer with time-wise periodic boundary conditions, *J. Heat Transfer* **101,** 244–248 (1979).
7. E. J. Hinch and G. Schubert, Strong streaming induced by a moving thermal wave, *J. Fluid Mech.* **47,** 291–304 (1971).
8. F. H. Busse, On the mean flow induced by a thermal wave, *J. Atm. Sci.* **29,** 1423–1429 (1972).
9. R. E. Young, G. Schubert and K. E. Torrance, Nonlinear motions induced by moving thermal waves, *J. Fluid Mech.* **54,** 163–187 (1972).
10. J. A. Whitehead, Observations of rapid mean flow produced in mercury by a moving heater, *Geophys. Fluid Dynam.* **3,** 161–181 (1972).
11. J. G. Georgiadis and I. Catton, Prandtl number effect on Bénard convection in porous media, *ASME J. Heat Transfer* **108,** 284–290 (1986).
12. M. M. Chen and J. A. Whitehead, Evolution of two-dimensional periodic Rayleigh convection cells of arbitrary wave-numbers, *J. Fluid Mech.* **31,** 1–15 (1968).
13. L. A. Segel, Non-linear hydrodynamic stability theory and its applications to thermal convection and curved flows in non-equilibrium thermodynamics. In *Variational Techniques and Stability* (Edited by R. J. Donnelly, R. Herman and I. Psigogine). University of Chicago Press, Chicago (1966).
14. T. Tomimura and M. Fujii, Laminar mixed convection heat transfer between parallel plates with localised heating, *Proceedings of the International Symposium on Cooling Technology for Electronic Equipment*, pp. 233–247. Honolulu (1987).
15. M. Hasnaoui, E. Bilgen, P. Vasseur and L. Robillard Mixed convection in a horizontal channel heated periodically from below, *Numer. Heat Transfer* **20,** 297–316 (1991).
16. A. Tangborn, A two-dimensional instability in a mixed convection flow with spatially periodic temperature boundary conditions, *Physics Fluids* **A-4,** 1583–1586 (1992).
17. C. Yücel, M. Hasnaoui, L. Robillard and E. Bilgen, Mixed convection heat transfer in open ended inclined channels with discrete isothermal heating, *Numer. Heat Transfer* **24,** 109–126 (1993).
18. M. Prats, The effect of horizontal fluid flow on thermally induced convection currents in porous medium, *J. Geophys. Res.* **71,** 4835–4838 (1966).
19. L. Robillard and K. E. Torrance, Convection heat transfer inhibition in an annular porous layer rotating at weak angular velocity, *Int. J. Heat Mass Transfer* **33,** 953–963 (1990).
20. E. R. Lapwood, Convection of a fluid in a porous medium, *Proc. Camb. Phil. Soc.* **44,** 508–521 (1948).
21. W. R. C. Phillips, *The Generalized Lagrangian Mean Equations and Stream wise Vortices-Near-wall Turbulence* (Edited by S. Kline). Hemisphere, New York (1988).
22. P. Cheng, Heat transfer in geothermal system, *Adv. Heat Transfer* **14,** 1–105 (1978).
23. J. P. Caltagirone, Thermoconvective instabilities in a horizontal porous layer, *J. Fluid Mech.* **72,** 269–287 (1975).
24. P. Ehrhard and U. Muller, Dynamical behavior of natural convection in a single-phase loop, *J. Fluid Mech.* **217,** 487–518 (1990).
25. D. A. Nield and A. Bejan, Internal natural convection: heating from the side. In *Convection in Porous Media*, Chap. 7, pp. 251–258. Springer, Berlin (1992).